1

Crystallization in Glass Forming Substances: The Chemical Bond Approach

Elena A. Chechetkina
Institute of General and Inorganic Chemistry of Russian Academy of Sciences, Moscow, Russia

1. Introduction

Glassy materials are strongly connected with crystallization or - more strictly - with the ability to *avoid* crystallization when cooling a melt. The more stable a supercooled liquid against crystallization, the higher its glass forming ability. It should be noted that almost every substance can be preapared in the form of amorphous solid by means of special methods of fast melt cooling (in the form of ribbons), evaporating (films), deposition (layers) and sol-gel technique (initially porous samples), etc. [1]. The resulting materials are often named "glass" (e.g., "glassy metals"), but they are actually outside the scope of this chapter. Here, we consider only typical inorganic glasses, such as SiO_2 and Se, which correspond to an understanding of glass as a *bulk non-crystalline solid prepared by melt cooling*. "Bulk" means a 3D sample having a size of 1 cm and larger, a condition that implies a cooling rate of about 10 K/s and lower. Despite the "technological" character of this definition, it is the most objective one, being free from the declared or hidden speculations about the nature of glass.

The theoretical background is given in Section 2, beginning with classical notions about crystallization in ordinary melts and the concept of the *critical cooling rate* (CCR), understood as the minimal cooling rate that provides the solidification of a melt without its crystallization. As far as any crystallization ability is reciprocal to a glass forming ability, one can evaluate a *glass forming ability* in terms of the CCR, using both crystallization theory and experiments. It will demonstrate a principal inapplicability of classical crystallization theory in the case of glass forming substances. As an alternative, we have developed a new approach based on the hypothesis of *initial reorientation*, considered as a specific pre-nucleation stage in a non-crystalline network. The classical model of a *continuous random network* consisting of common covalent bonds (two-centre two-electron, 2c-2e) is modified in two respects. First, we introduce *hypervalent bonds* (HVB) in addition to covalent bonds (CB); and besides, such bonds can be transformed into one another (CB↔HVB). Second, the elementary acts of bond exchange are in spatiotemporal correlation, thus providing a *bond wave* by means of which the collective processes - including initial reorientation and further crystallization - may occur. A bond wave also means a non-crystalline order of hierarchical character: from the well known short-range order (it changes in the vicinity of HVB), through the well known but poorly-understood medium-range order (in the limits of the wavefronts populated with HVB), to the non-crystalline long-range order generated by bond waves. Insofar as bond waves change their parameters and direction during melt cooling, being frozen in solid glass, the non-crystalline long-range order depends not only

on the substance under consideration but also on the sample prehistory. This is a principal distinction from the ordinary long-range order in crystals, which is strictly determined for a given substance at a given temperature. As such, the problem of crystallization in glass can be considered as a competition between two types of order, and hypervalent bonds and their self-organization in the form of a bond wave play a central role in this process.

In Section 3 and Section 4, original crystallization experiments based on the above approach are described. In Section 3, we consider crystallization in **solid Se-X** glasses, in which additions of a different chemical nature (X = Cl, S, Te, As, Ge) are used. A set of properties, including the abilities of nucleation and surface crystallization, was investigated based upon the composition for each series. A strong *non-linearity* was found in the region of small additions $N<N^*$ (concentration N^* depends on the nature of X), which is discussed in terms of the bond wave interaction with foreign atoms also existing in a hypervalent state. Finally, in Section 4, original experiments on the crystallization of **softening Se-X** glasses in an **ultrasonic field** are presented. In softening glass, bond waves are refrozen and an ultrasonic field can act as an *information field* for them; in our case, a US-field can give a predominant direction for the crystallization process. Actually, the resultant glasses become *anisotropic*, the anisotropy also being non-linear in respect to the composition.

Thus, starting from the classical approach operating with a 3-step process of crystallization (sub-critical unstable nucleation, stable nucleation, crystal growth), fluctuations, atomic jumps, atomic/geometrical structure, one-type bonding and one-type long-range order, we pass to a strange picture of mixed bonding, bond waves, "wavy" long-range order and glass as a self-organizing system.

The text is intended for a wide audience. The readers from the field of glass are invited to meet with new experiments and new ideas. For beginners – let us now enter into the mysterious world of glass!

2. Crystallization in supercooled glass forming liquids ($T>T_g$)

2.1 Critical cooling rate

The idea of the CCR as a measure of a glass forming ability seems to be trivial, but it remained in the shadows up until 1968, when *Sarjeant & Roy* [2] emphasized "the concept of '*critical quenching rate*'… defined as the cooling rate below which detectable crystalline phases are obtained from the melt" and proposed the first theoretical expression for the CCR in the form of:

$$Q_c = 2.0*10^{-6}*(T_m)^2*R/V*\eta \quad (1)$$

Here T_m is the melting point, η (poises) is the viscosity at T_m and V is the volume of the "diffusing species". The main problem is the evaluation of V, which needs "an extreme simplification and interaction of many parameters involved" [2]. Nevertheless, it is seen in **Table 1** that the values thus obtained are in agreement with the later estimations of the CCR [3-5] using the equations of classical crystallization kinetics.

Strictly specking, it is easy to fit into the "classical" gap [3-5] that extends for orders in magnitude. More interesting is the tendency for this gap, $\Delta|\lg Q_c|$, to be especially wide just for glass-formers (G). It is seen in **Fig.1** that in glass forming substances ($Q_c<10^2$ K/s by definition) the difference $\Delta|\lg Q_c|$ increases when Q_c decreases, i.e., the larger the gap, the

greater the glass forming ability. Moreover, and to the contrary, for non-glass forming substances (Q_c>10^2 K/s), there is no relation between Q_c and its variation, the latter actually being the same for all non-glass formers.

Substance	T_m, K	lgQ_c(K/s)				$\|\Delta \lg Q_c\|$
	[4]	[2]	[3]	[4]	[5]	
SiO_2 (G)	1993	+0,6	-3,7	-1	-2,9	4,3 (G)
B_2O_3 (G)	733		-1,2	-16	-7,3	8,7 (G)
GeO_2 (G)	1359			-11	-2,9	9,8 (G)
P_2O_5 (G)	853			-23	-5,9	17,1 (G)
As_2O_3	1070			+7	+4,1	2,9
H_2O	273	+7,2	+7	+12	+10,4	5,0
Salol (G)	316.6		+1,7	-15		13,3 (G)
Ethanol	159			-2	+1	3,0
Glycerin (G)	293			-40	-7,9	32,1 (G)
CCl_4	250,2			0	+5,2	5,2
C_6H_6 (G?)	278,4			-14	+4,9	18,9 (G?)
BeF_2 (G)	1070			-3	-4,0	1,0 (G)
$ZnCl_2$ (G)	548			-21	-4,4	16,6 (G)
$BiCl_3$	505			+7	+5,5	1,5
$PbBr_2$	643			+3	+6,3	3,3
NaCl	1073	+9,1		+10	+8,4	1,6
$NaNO_3$	580			+5	+7,0	2,0
$NaCO_3$	1124			+3	+5,0	2,0
$NaSO_4$	973			+10	+7,4	2,6
$NaWO_4$	1162			+7	+8,4	1,6
Ag	1234	+8,0	+10	+8	+9,3	1,3
Cu	1356			+9	+8,5	0,5
Sn	505,7			+2	+7,9	5,9
Pb	600,7			+10	+8,7	1,3

Table 1. The calculated CCRs among the groups of oxides, substances with hydrogen bonding and/or organic glass formers, halides, sodium salts and metals. The "G" in brackets indicates a well-recognized glass former.

One should note the absence of benzene (see C_6H_6 in Table 1) in Fig.1. This is a result of the outstanding disagreement in the evaluations of its CCR: benzene looks like an excellent glass former after [4], but after [5] it is a non-glass former. When lgQ_c=+4,9 after [5], the point for difference $\Delta|\lg Q_c|$=18,9 is dramatically lifted above the "amorphous line"; however, if one takes lgQ_c=−14 after [4], the point falls far below the correlation line for glass formers.

The Qc interval in Fig.1 extends for 19 orders in magnitude. The practical interval is far narrower. For glasses, there are three useful CCR points: the glass definition limit Q_c=10^2 K/s, which corresponds roughly to a quenching of a 1 cm^3 sample in water with ice, the rate of 10 K/s corresponding to quenching in the air, and the rate of 1-10^{-2} K/s corresponding to free cooling in a furnace. Therefore, the extremely large negative values of lgQ_c(K/s) in Table 1 - such as -16 for B_2O_3 or -23 for P_2O_5 [4] - only display an extremely high glass forming ability, i.e., the ability for very slow cooling in a furnace, a feature which provides the opportunity to obtain very massive articles, such as lenses for telescopes. For amorphous

materials (Q_c>10^2 K/s), the experimental limit is about Q_c=10^6 K/s, which corresponds with the preparation of amorphous ribbons, namely the 2D case. The calculated value of Q_c=10^8-10^{10} K/s displays only an extra low amorphization ability of a substance, which cannot be obtained by melt cooling at all. This is really the 1D case, when the amorphous film is prepared by evaporation onto a cold substrate.

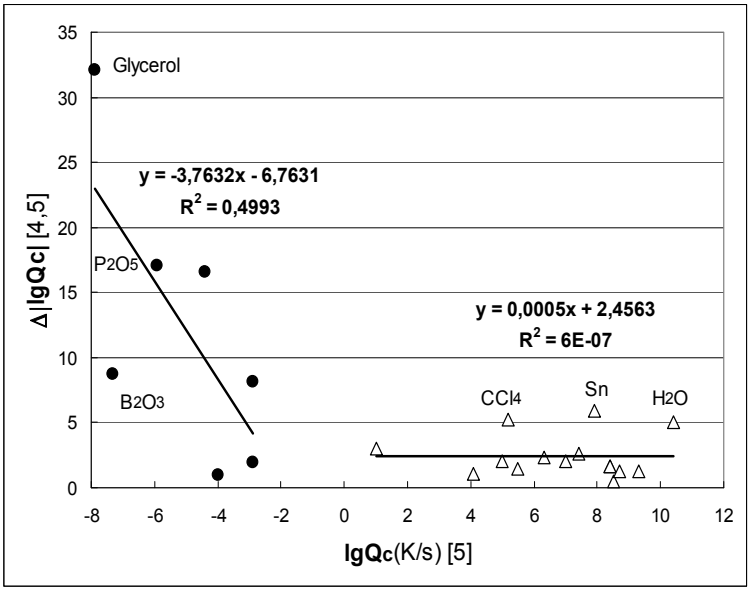

Fig. 1. The absolute difference between the calculated values of the CCRs from [4,5] as a function of the CCR value after [5]. The data is from Table 1.

Based on the tendency in Fig.1, one can conclude that the greater the glass forming ability, the more problematic the application of the classical theory of crystallization. In reality, in the case of a lithium disilicate glass it was shown that "not only do all forms of classical theories predict nucleation rates many orders in magnitude smaller than those observed, but also the temperature dependence of the theoretical rate is quite different from that observed" [6]. Thus, crystallization in glasses needs special methods, both theoretical and experimental.

Although there are many experimental works on the crystallization of glass and glass forming liquids, only a few of them concern the CCR. The known evaluations of Q_c in oxides [7-11] and chalcogenides [12-16] are made by either a direct method covering a relatively small lgQ_c interval (e.g., from -2 to +4 after [7-10]), or indirect methods. By 'indirect' is meant that the crystallization data corresponding to some extent of crystallinity α~0,01-0,1 is recalculated to a much lower α corresponding to Q_c (usually to α=10^{-6} [15-16]) using equations of the *Kolmogorov-Avrami* type. However, the applicability of such equations in an extra low α region is also under question. Thus, it is not surprising that interest in the investigation of the CCR is low at present. The reader can find a critical review of the "golden age" of the CCR in the last third of the Twentieth Century in our monograph [17]. The main result of this period seems to be the formulation of new problems concerning glass forming ability.

The general question is what is meant by the demand of melt cooling "without crystallization"? After *Vreeswijk et al.* [4] glass is considered as being partially crystallized even one critical nucleus is formed; this is a **theoretical** limit for estimation of the Q_c value. Later, *Uhlmann* [3] proposed the crystalline fraction $\alpha=10^{-6}$ for the **experimentally** detected limit, and *Ruscenstein & Ihm* [5] proposed $\alpha=10^{-4}$ for a more convenient **practical** limit. Obviously, the lower α, the higher Q_c for a given substance. However, when comparing the calculation results in Table 1 - we see that there is no a relation between the crystalline fraction permitted (α increases from [4] to [5]) and the corresponding Q_c values. Thus, classical crystallization theory needs serious reconsideration for glass forming substances.

2.2 Induction period, transient effects and initial reorientation

The critical nucleus - arising when overcoming the "thermodynamic" barrier W* with the following steady-state nucleation of the *I(T)* frequency and the steady-state crystal growth of the *u(T)* rate - forms the basis of classical crystallization theory. The critical nucleus is considered as the cause of the *induction period* observed in the process of crystallization. It is unclear, however, to what extent the classical notions are true for glass forming substances. In order to test the assumption about steady-state nucleation, *Kelton & Greer* [18] have analysed the data for lithium disilicate (a typical glass former) and two metallic "glasses" ('amorphous metal' would be a more appropriate term). When the authors introduced the time-dependent nucleation frequency *I(τ,T)*, they revealed the so-called *transient effects* which occurred to be most significant only for typical glass. Transient effects, together with the fact that "*even small uncertainties of material parameters can introduce uncertainties of several orders in magnitude in the calculated nucleation frequency*" [18], make the application of classical crystallization theory problematic in the case of glass forming substances.

On the other hand, from the beginning of the 1980s onwards, we have developed an alternative approach for the prediction of glass forming ability in relation to crystallization ability. This approach is based on *Dembovsky's* "empirical theory of glass formation" [19], by which one can calculate the dimensionless glass forming ability, which was transformed further into an energetic barrier for crystallization E_{cr} [20]. The next stage was the transformation of the semi-empirical E_{cr} (enthalpy) to the barrier $\Delta G^{\#}$ (free energy), and finally $\Delta G^{\#}$ to the CCR measure V_m [21,22]. The reader can find a complete calculation scheme for V_m in [17; p.145] or [23; p.105]. Two points of this CCR are of special interest.

First, in order to calculate V_m, one needs *no kinetic parameters*, such as a coefficient of diffusion and/or viscosity. Instead, we use only the phase diagram of a system (in order to determine the liquidus temperature for a related unit: an element, a compound, an eutectic or else an intermediate), the first coordination number (presumably, in the liquid state at around T_m) and the averaged valence electron concentration (e.g., 6 for Se, 5.6 for As_2Se_3, 5.33 for SiO_2, etc.).

Second, the barrier $\Delta G^{\#}$ was attributed to a special pre-crystalline ordering named the *initial reorientation* (IReO), which is postulated as the stage after which crystal nucleation and growth is possible [21]. IReO means that neither nucleation nor crystal growth can proceed in a non-oriented - i.e., a truly "amorphous" - medium. Since IReO is a simple activation process with the $\Delta G^{\#}$ barrier, the reoriented fraction increases exponentially with time, as the dotted line in Fig.2 shows.

States:

(1) $A \rightarrow A_0 \rightarrow A_{Nu}$

(2) $A_0 \rightarrow A_{Cr}$

(3) $A \rightarrow A_0 \rightarrow A_{Cr}$

Barriers:

(1) $\Delta G^{\#}$; $(W^* + \Delta G^{\#})$

(2) $\Delta G' \rightarrow \Delta G''$

(3) $\Delta G^{\#}$; $\Delta G''$

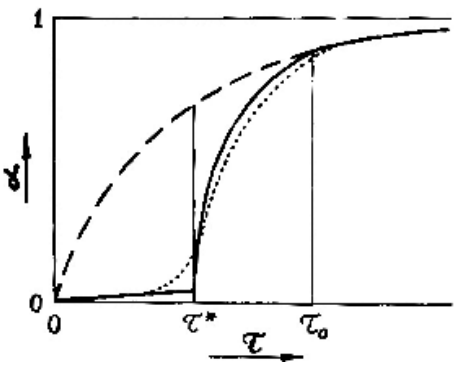

Fig. 2. Isothermal crystallization after [21]: the dotted curve describes the development of the reoriented non-crystalline fraction; the solid line is the model temporal dependence of the extent of crystallinity α; the pointed curve is a real crystallization process.
Atomic states: **A** is the initial truly "amorphous" state for a species in a supercooled liquid or glass; $\mathbf{A_0}$ is the reoriented state; $\mathbf{A_{Nu}}$ is the state of the crystal nucleus; $\mathbf{A_{Cr}}$ is the state of the growing crystal.
Barriers: $\Delta G^{\#}$ is the initial orientation; W^* is the critical nucleus; $\Delta G'$ is the steady-state nucleation; $\Delta G''$ is the crystal growth.

The three intervals in Fig.2 correspond to an *induction period* at $0<\tau<\tau^*$, a *transient period* at $\tau^*<\tau<\tau_0$ and a *saturation* at $\tau>\tau_0$. At first, the reoriented areas are relatively small and/or disconnected, such that only nucleation can proceed. Although nucleation is permitted, the extent of the crystalline fraction (the solid line) is negligible when compared with the reoriented fraction (the dotted line). At the moment τ^*, the reoriented areas become large enough and/or percolated so as to permit not only nucleation but also crystal growth, using both the arising and newly existing portions of the reoriented species. In this *transient* region $\tau^*<\tau<\tau_0$, crystallization slows gradually and at τ_0 it becomes limited by the process of initial reorientation when each new portion of the reoriented species joins directly to the growing crystals.

One should note in Fig.2 the well known barriers G', G'' and W^*. Fortunately, the problems with these barriers (e.g., varying G' after [18] or an anomalous increase of W^* with a decreasing temperature at about T_g [24]) are outside of our method for the estimation of the CCR since V_m relates only to the initial reorientation stage with the $\Delta G^{\#}$ barrier which determines the boundary between glassy and crystalline states. Thus, V_m is the *upper* theoretical limit for the CCR and in this sense V_m satisfies the condition set by *Vreeswijk et al.* [4] concerning the absence of even one critical nucleus when determining the CCR.

By 'initial reorientation' is meant some kind of order. Interestingly, the notions concerning pre-crystalline ordering in glasses appear consistently in the literature. One can see the IReO in a real SEM image, which is interpreted by the authors as "a pre-crystallization stage, in which glass matrix becomes inhomogeneous, forming nano-sized volumes" [25]. Indirect evidence of the IReO is seen in the conclusion that "glass-transition kinetics can be treated as pre-crystallization kinetics" [26] as well as in the models of "dynamic heterogeneity" in an amorphous matrix before its crystallization [27-29]. The problem is that both "dynamic heterogeneity" and "initial reorientation" are the only terms that need decoding.

2.3 Glass structure, hypervalent bonds and bond waves

The theory of glass structure was actually formed at 1932 when, beginning with the words "*It must be frankly admitted that we know practically nothing about the atomic arrangement in glasses,*" the young scientist *Zachariasen* proposed his famous model of a **continuous random network** (CRN) [30]. This network consists of covalent bonds, - the same as that in a related crystal - and the only difference is the "random" arrangement of the bonds in CRN in contrast with their regular arrangement in a crystalline network. As far as the atomic arrangement in CRN is determined by the arrangement of chemical bonds, one might suppose that only chemists - who deal with chemical bonds - would play a leading role in the further development of the CRN model. However, the development was directed in another "physical" way. As a result, the chemical bond is present in contemporary glass theory in the form of "frustration", "elastic force" and rigid "sticks" connecting atoms-balls, etc., but not as a real object with its own specificity. We think that a pure "physical approach" opens a rich field for theoretical speculation, rather than clarifying the nature of glass. For example, to understand glass transition, the analogues with spin glasses, granular systems and colloids are used (e.g., see the excellent review [31]), although any similarity in behaviour does not mean that the similarity is the reason behind that behaviour.

One can find, however, deviations from the main "physical" stream of glass science, even among physicians. As a fresh example, we may cite that: "*It is widely believed that crystallization in three dimensions is primary controlled by positional ordering, and not by bond orientational ordering. In other words, bond orientational ordering is usually considered to be merely a consequence of positional ordering and thus has often been ignored. … Here we proposed that bond orientational ordering can play a key role in (i) crystallization, (ii) the ordering to quasi-crystal and (iii) vitrification*" [29]. Although this is a rare case, it may be a sign that the need for a chemical approach is now stronger.

Our goal was to return the chemical bond - as chemists know it - to the theory of glass. As far back as in 1981, *Dembovsky* [32] has connected the experimental fact of an *increased* coordination number in glass forming melts with the model of *quasimolecular defects* (QMD) following *Popov* [33] for the creation of the chemical-bond basis for glass theory. The principal feature of a QMD is its hyper-coordinated nature, a property that provides for the connectivity of a covalent network even at melt temperature, thus resulting in high melt viscosity, which is a characteristic property of a glass forming melt. QMDs in a non-crystalline network can also explain general features of glass [34-38]. The problem is that the concentration of QMDs should be high enough, especially in a glass forming liquid, to provide these features. Therefore, we have quickly substituted the initial term QMD (quasimolecular *defect*) for TCB (three-centre *bond*) and then, being based on a special quantum-chemical study (see the reviews [39] for chalcogenide glasses and [40] for oxide ones), TCB for HVB, **hypervalent bond.** TCB is only a particular case of HVB, which is rarely realizes in glass. For example, in the simplest case of Se not TCB, having two three-coordinated atoms (-Se<) and one "normal" two-coordinated atom (-Se-) [33], but a four-coordinated atom (>Se<)was revealed [41]. Thus, we have introduced *alternative bonds* into CRN, the bonds whose concentration is commensurable with that of ordinary covalent bonds constituting classical CRN.

The term "hypervalent", which was introduced by *Muscher* in 1969 [42], has a long and controversial history, beginning from the 1920s up until the present (see [43] for an introduction). Currently, a large number of hypervalent molecules is known, and various methods of their theoretical description exist. For a long time, one of the most popular was

the *Pimentel's* model [44] of the electron-rich three-centre four-electron (3c-4e) bond; this model was used by *Popov* to construct his "quasimolecular defect" in a covalent network of Se glass [33]. The principal step made by *Dembovsky* was in the understanding of QMD not as a "defect" but as the second type of bonding in a glassy network, the first being a common two-centre two-electron (2c-2e) covalent bond. The next step was made by means of *ab initio* quantum-chemical modelling, which reveals various metastable hypervalent configurations - configurations in which a central atom has more bonds with its neighbours than the "normal" surrounding covalent species - in glasses. We use the term *hypervalent bonds* in order to emphasize the additional bonding state in non-classical CRN, and so the additional structure possibilities in it. This network is not "random" now.

Three types of order can be realized in such a mixed network. When the diffraction pattern of glass is transformed into a radial distribution function one can observe the so-called *short-range order* (SRO) extending to the limits of at least two coordination spheres around an arbitrary atom. The peak's position relates to the distances between the nearest neighbours and the peak square to the number of these neighbours. The SRO in glass is close (but not coinciding completely!) with the SRO in a counterpart crystal, with both SROs being determined by a bond length (first distance), valence (first coordination number) and valence angles (second coordination sphere). The SRO is the basis for a conventional continuous random network, but the problem is that a CRN consisting of covalent bonds cannot exist because of the rigid and directional character of the covalent bond. When moving from the first atom, the stress due to bond distortion accumulates rapidly up to a critical value above which the covalent bond should be destroyed (the covalent bond limits are known in the chemistry of related compounds). This means that a real CRN should contain either internal fractures (however, glass is known to be an optically transparent and mechanical stable material) or additional "soft" regions for relaxation. These regions are provided by HVB and are soft and flexible when compared with covalent bonds.

The next step of order which surely exists in a non-crystalline state is the so called *medium-range order* (MRO), which is observed directly in the diffraction pattern of glass or glass forming liquids in the form of the well known *first sharp diffraction peak* (FSDP). It is a very narrow (for an amorphous state) peak located at about Q_1=1-1,5Å^{-1}; the peak position and intensity depend upon the chemical composition, temperature and pressure (see [45,46] for a review). The two generally accepted parameters of the MRO are the correlation length $d=2\pi/Q_1\approx$6-4Å and the coherence length $L= 2\pi/\Delta Q_1\approx$10-20Å, where ΔQ_1 is the FSDP half-width.

The nature of the FSDP/MRO is debatable at present. Our interpretation of the MRO is based on hypervalent bonds and their collective behaviour in the form of a *bond wave*, which is illustrated in **Fig.3**.

A bond wave is the spatiotemporal correlation of elementary acts of the reversible transformation of a covalent bond and a hypervalent bond: CB↔HVB. A snapshot of a bond wave, which spreads in the Se-like network, is shown in the left part of Fig.3. The wavefronts represent equidistant layers populated with hypervalent bonds (they are modelled by TCB in Fig.3), and so the correlation length $d=2\pi/Q_1$ roughly corresponds with the HVB length. The layers give a true Bragg reflex at $Q_1=2\pi/d$, so the FSDP intensity and the FSDP width depend upon the number of these reflecting layers and their reflection ability, with both depending on the temperature.

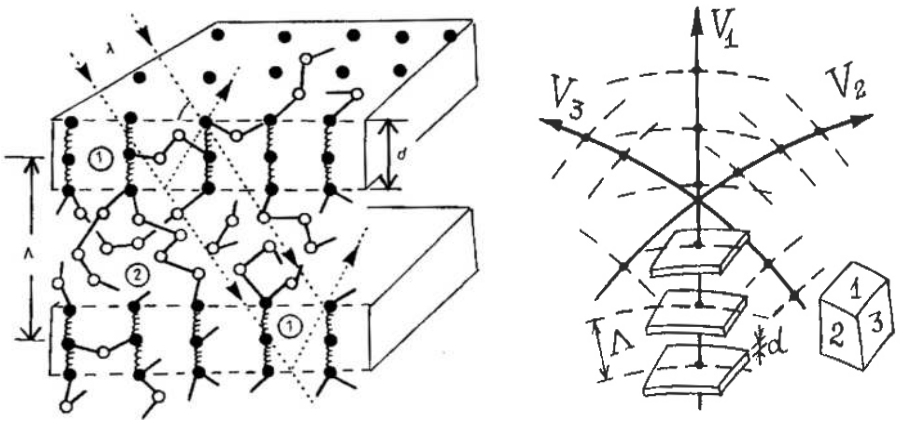

Fig. 3. Bond waves after [46]. On the left: two adjacent wavefronts – layers "1" populated with a HVB (here modelled by a TCB: black atoms linked by spring) together with a CRN "2" between the layers (here an Se-like CRN, which consists of white atoms, each having two covalent bonds as shown by the lines). On the right: the intersection of three bond waves, which gives the 1-2-3 elementary cell.

A bond wave with a Λ wavelength represents a totality of d-layers, and the totality represents a periodic structure of the Λ period. Thus, there appears a Λ-lattice and a corresponding *long-range order* (LRO) in glass. This order is, in some respects, similar to the smectic-type LRO; however, in glass - in contrast with liquid crystal - there are two types of bonding species in the layer and the d-layers themselves are punctuated with thick pieces of the CRN. Such long-range periodicity is "invisible" to ordinary X-ray analysis, by which one can see a CRN (in the form of the peaks in the radial distribution function) and d-layers (in the form of a FSDP in an initial diffraction pattern), but not the Λ-lattice. The reflex from the Λ-lattice should be disposed in the 0.01-0.001$Å^{-1}$ range, which is inaccessible to the usual X-ray techniques. Thus, special techniques (e.g., those using synchrotron radiation) are needed to see a LRO in glass.

One can note that the layer structure shown in the left side of Fig.3 is *anisotropic*, while glass is known to be an *isotropic* medium. Note, however, that anisotropic glasses can also be prepared (our own experiments of this sort will be considered below). The generally observed isotropic behaviour of glass means the *solitonic* behaviour of bond waves, i.e., the waves ability to intersect each other without distortion, as is shown on the right in Fig.3. One wave propagating through a CRN with the velocity V_1 forms the layer structure, two waves (V_1+V_2) create the columnar structure, and three waves (V_1+V_2+V_3) correspond to the cellular structure, which is isotropic on the macroscopic scale. The factors which govern bond waves and, consequently, the structure that they form, can be divided into internal (chemical composition, temperature, pressure) and external (flows of energy and/or information) categories.

As far as the elementary act CB↔HVB is considered to be a thermally activated process, both the wave frequency and the HVB concentration increase with temperature, while the wavelength Λ decreases [47]. Thus, when approaching the glass transition temperature T_g, the interlayer distance Λ becomes so large that the correlation between the layers/wavefronts becomes impossible, although the intimated HVBs within the layers continue to "feel" each

other. This means that a 3D bond wave (Fig.3, right side) stops its propagation through the structure and the 2D bond wave within the stopped d-layers (Fig.3, left side) remains mobile. Thus, the glass transition can be considered as a 3D→2D bond wave transition [48].

As far HVBs represent active sites in the mixed CB/HVB network, one should distinguish between the processes above and below T_g. More specifically, the abovementioned pre-nucleation stage in the form of initial reorientation (IReO) proceeds within the stopped d-layers below T_g and only after the reconstruction of the layers can it penetrate into the CRN: the process is slow and has an induction period (see $\tau<\tau_0$ in Fig.2). Above T_g, where the 3D bond waves exist, the d-layers pass through every structure element: the induction period is short, if it even exists, and the process is much faster and homogeneous.

Crystallization is not the first property considered by means of the bond wave model. Earlier, this model was applied successively for the interpretation of the thermodynamic features of glass forming substances [49], characteristic glass fractures [50], the first sharp diffraction peaks [46] and the temperature dependence of viscosity [51]. Unfortunately, there are only interpretations and so far there is no direct evidence of bond waves at present, i.e., the direct observation of a Λ-lattice in a structural experiment. Instead, we performed a computational experiment [52], presented in **Fig.4**, in which we intended to investigate the ability of the HVB for association – this property alone is a necessary requirement for the existence of a bond wave.

In model clusters like those shown in Fig.4, a single HVB looks like a "defect" embedded into an ordinary continuous random network (CRN). A single HVB was shown to be a low-energy "defect" (compare 0,3 eV for Se_4^0 [41], with 2 eV needed to generate a broken bond $2Se_2 \rightarrow 2Se_1$ or with 1 eV proposed for the so called "valence alternation pair" $Se_3^+Se_1^-$ after [53], the index below is the coordination and the index above is the charge). Nevertheless, even such low-energy defects cannot ensure the above-mentioned over-coordination in glass (there needs to be ~1% for four-coordinated atoms) and especially so in a melt (ten%) [37]. From Fig.4, it follows that the associated HVBs are much more stable, so that even *negative energy* regions can arise in a CRN for a definite HVB arrangement (SS).

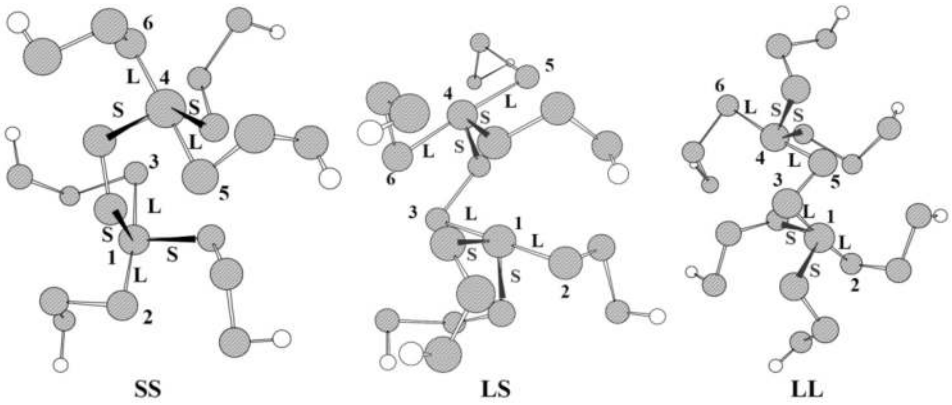

Fig. 4. Quantum-chemical modelling of the HVB interaction in Se after *Zyubin & Dembovsky* [52]. The cluster energies are **−0.16 eV** (SS), +0.08 eV (LS) and +0.09 eV (LL); the notations correspond with the mutual orientation of short (S) and long (L) pairs of bonds surrounding each Se_4^0 atom (1 or 4). The white spheres are the hydrogen atoms terminating the clusters.

In this way, not only is a principal ability to form a bond wave justified, so is the connection of a *structural order* due to a Λ-lattice with an "*energetic order*", which is based on the intuitive belief that the more structurally ordered substance has the lower energy (with other conditions being equal). As such, the processes of the crystallization of glass, both below and above T_g, can be considered as the competition of two types of order: a crystalline long-range order and a specific non-crystalline long-range order, provided by hypervalent bonds and bond waves. In what follows, these notions are tested by means of special crystallization experiments.

3. Crystallization in solid glass ($T<T_g$)

3.1 The composition dependent rate of nucleation

For these experiments, we chose selenium as the simplest one-element glass; the additions, with various valence abilities, were introduced into the Se matrix, giving five series of Se-X (X = S, Te, As, Ge, Cl) with a varied but relatively low concentration of the second component. The as-prepared samples were cylinders measuring 25 mm in diameter and 15 mm in height; the two cylinder ends were polished. The optical transmission and ultrasonic velocity were measured through the ends; the X-ray fluorescent spectra were measured from the end surface.

The as-prepared samples were quite transparent, actually having the same value of transmission at 1000 cm^{-1} (this value, which corresponds with entry into the so-called "window of transparency" for selenide glasses, we shall call *transparency*) of around 60%, a value that is typical for chalcogenide glasses of high quality for the given thickness of 15 mm. The two other properties (V and r) investigated in the fresh glasses, however, were strongly dependent upon composition, as is seen in **Fig.5**. Note that the both properties are *macroscopic* in character. The ultrasound velocity, V, characterizes the elastic ability of the Se-based network. The relative intensity of the X-ray fluorescence, $r=S_{val}/S_{char}$ (S_{val} and S_{char} are the integral intensities of the $K_{\beta 2}$ and $K_{\beta 2}$ emission lines for Se, the first corresponding to the 4p→1s transition from a valence band and the second to the characteristic 3p→1s inner transition for Se), belongs to the totality of selenium atoms, reflecting the average valence state for Se.

We see a strong non-linear character for all of the dependencies in Fig.5. The two upper cases of Se-Te and Se-S seem to be the most surprising because S and Te belong to the same VI group of the Periodic Table, having the same number of covalently bonded neighbours per atom. Additionally, the Se-Te phase diagram is a simple "fish", which corresponds with the discontinuous series of liquid and solid solutions. However, the *metastable phase diagram* (remember that glass is formed far below the melting point from a metastable liquid) has a "two-fish" form, with "two series of solid solutions meeting at 96.8 at%Se [i.e., 3.2 at%Te – ECh] and temperature 180°C" [55].

Note that the Se-Te glasses display extrema in the 1-4%Te range for the other composition-property dependences, e.g., for electrical and crystallization properties [56] and for the glass transition temperature [57]. *Dembovsky et al*. [58] have also revealed non-linearity when investigating crystallization kinetics in Se-Te glasses in the 0-5% range. In **Fig.6**, the data for CCRs calculated with the use of the data obtained is shown; one can see not only the conditional character of the CCR, the composition dependence of which depends on the chosen α, but also the non-linearity of $Q(N)$ for every chosen extent of crystallinity with the extrema located in the region 1-5%Te. Note that our calculation of the CCR in the form of V_m

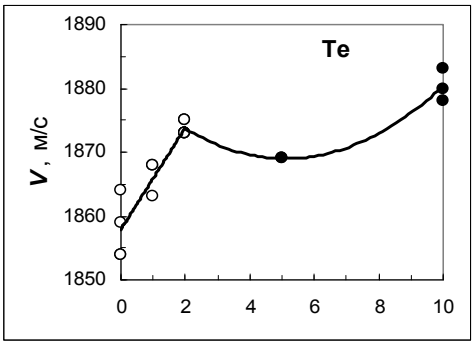
Te
V, м/с
1890
1880
1870
1860
1850
0
2
4
6
8
10

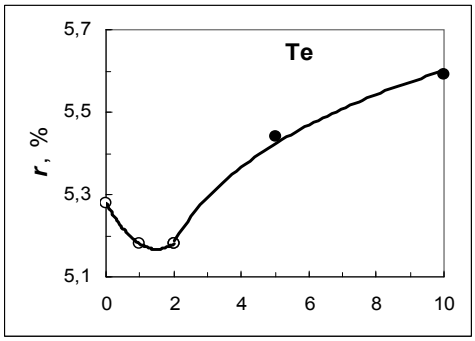
Te
r, %
5,7
5,5
5,3
5,1
0
2
4
6
8
10

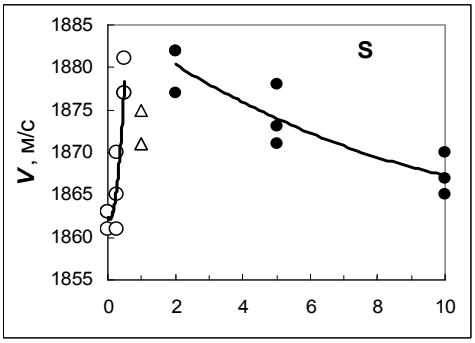
S
V, м/с
1885
1880
1875
1870
1865
1860
1855
0
2
4
6
8
10

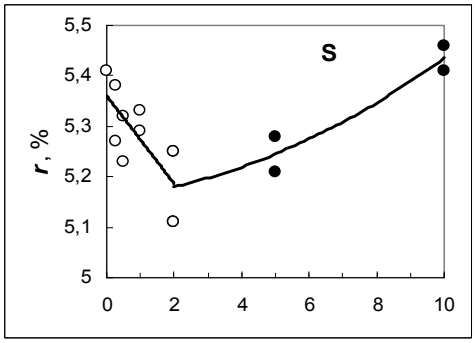
S
r, %
5,5
5,4
5,3
5,2
5,1
5
0
2
4
6
8
10

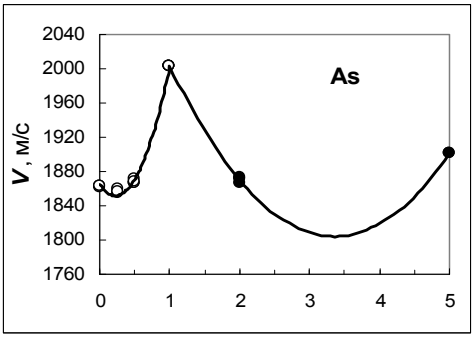
As
V, м/с
2040
2000
1960
1920
1880
1840
1800
1760
0
1
2
3
4
5

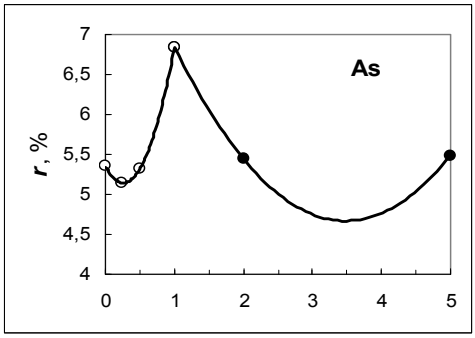
As
r, %
7
6,5
6
5,5
5
4,5
4
0
1
2
3
4
5

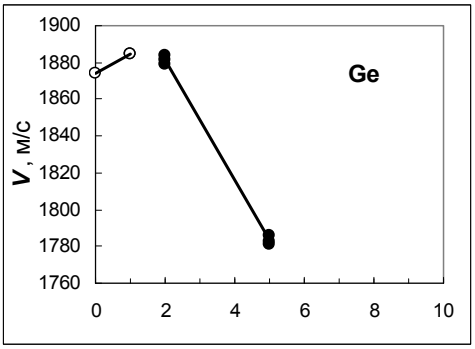
Ge
V, м/с
1900
1880
1860
1840
1820
1800
1780
1760
0
2
4
6
8
10

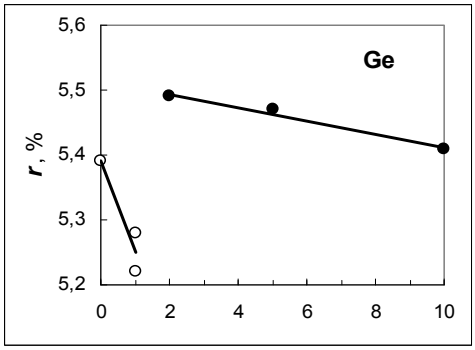
Ge
r, %
5,6
5,5
5,4
5,3
5,2
0
2
4
6
8
10

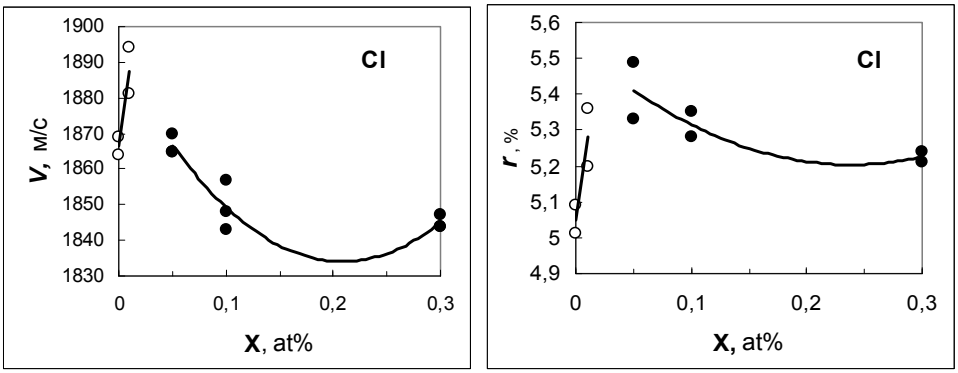

Fig. 5. Longitudinal ultrasound velocity (V) and relative intensity of X-ray fluorescence from the Se valence band (r) in the as-prepared Se-X glasses after [54].

[21,22], which corresponds to the pre-crystallization IReO stage, really represents the upper limit for the CCR, but only outside the non-linearity range. Remember, however, that when calculating V_m we only take into account the *equilibrium* fish-like phase diagram, whereas real glass relates more to metastable diagram(s) with peculiarities at about 5%Te.

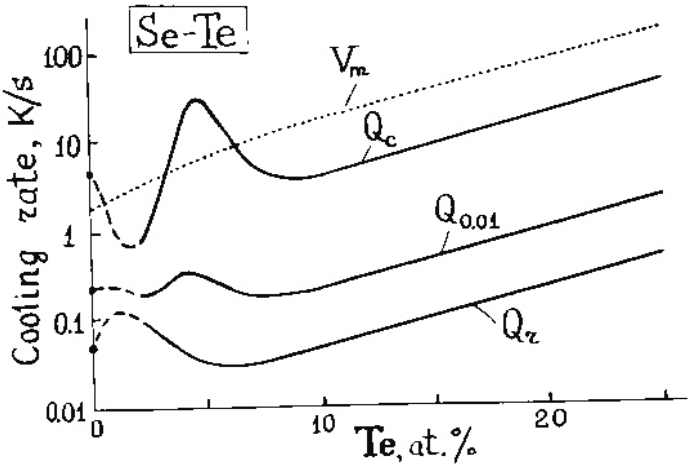

Fig. 6. Critical cooling rates (CCRs) in the Se-Te system after [58]. Q_r, $Q_{0.01}$ and Q_c correspond to the crystalline fraction α=0,63; 0,01 and 10^{-6} respectively. V_m is our calculation after [21,22], without the use of crystallization data.

The Se-S series in Fig.5 looks similar to Se-Te, although one can propose a more complex behaviour below 2%S, which can be compared with a more complex equilibrium Se-S phase diagram [59] in contrast with the simple "fish" for Se-Te.

In the Se-As and Se-Ge series, the additions belong to other groups of Periodic Table (IV for Ge and V for As), so one can expect another property-composition behaviour. Accordingly,

the *V(N)* and *r(N)* dependencies change in the same way in Se-As glasses (maximum on the both), in contrast with the behaviour in Se-Te and Se-S glasses, which display a maximum on *V(N)* and a minimum on *r(N)*. Although Se-Ge glasses are similar to Se-Te as concerns the maximum on *V(N)* at 2%Ge and the minimum on *r(N)* at about 1%Ge, the extrema in Se-Ge are much sharper and there is different post-extreme behaviour in Se-Ge as compared with Se-S and Se-Te.

The Se-Cl glasses are of a special interest because, in contrast with the above four additions which belong to the well recognized glass forming Se-X systems, chlorine in *not* a glass forming addition for Se. It is usually assumed that Cl can only break the Se-Se bonds, thereby decreasing viscosity and thus the glass forming ability. In fact, Se-Cl glasses can be only prepared in the 0-0.3%Cl range, but in other respects the Se-Cl series demonstrates the same behaviour: the as-prepared Se-Cl glasses are quite transparent (about 60%) and their properties are strongly non-linear (see Fig 5, at the bottom).

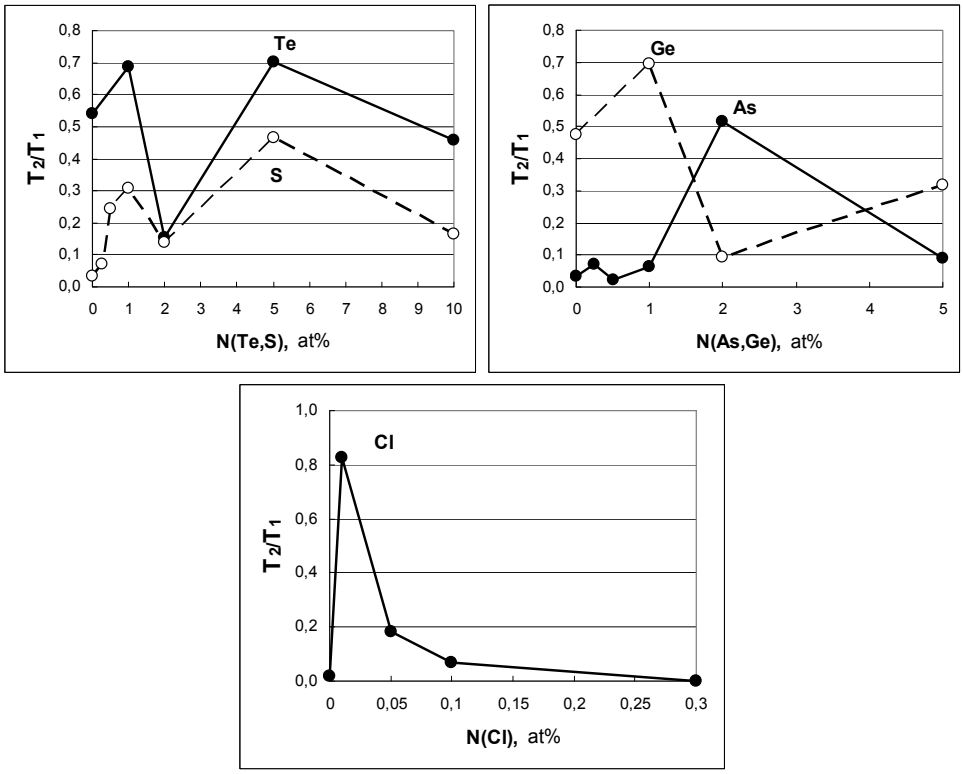

Fig. 7. Darkening in Se-X glasses after 5-year ageing at room temperature [60]. Here, *T* is the transparency (optical transmission at 1000 cm^{-1}); index "1" refers to the as-prepared glass and "2" to the aged glass. The unchanged transparency, i.e., the absence of darkening, corresponds to $(T_2/T_1)=1$ and complete darkening to $(T_2/T_1)=0$.

Next, the five series of glasses were stored for 5 years at room temperature, which is somewhat below the glass transition temperature ($T_g \approx 35^oC$ for Se). In accordance with the

expected crystallization, the **aged glasses** became less transparent, but not to the same extent. It can be seen in **Fig 7** that the transparency shows a non-linear character, like that shown in Fig.5 for ultrasound velocity and electron emission from the valence Se band. Thus, one can suppose that even in fresh Se-X glasses the special regions of initial reorientation (IReO) for further crystallization have been developed. These regions manifested themselves in *V(N)* and *r(N)* in Fig.5, but not in the transparency because the IReO regions were congruently inserted into a glassy matrix. During the process of ageing, the IReO regions are transformed into crystalline regions and so become visible due to light scattering from new crystal/glass boundaries.

The question is: what stage of crystallization do we observe in the aged glasses? The X-ray pattern of the aged samples usually looked like a wide hill of a low intensity; only the darkest samples display very weak crystalline peaks on the hill. Thus, because of the low extent of crystallinity (usually lower than 1%) together with the considerable darkening, we can conclude that by the optical transmission method we can observe the *nucleation stage* of crystallization. Next, from Fig.7 one can conclude that compositions of 1%Te and 5%Te, 5%S, 1%Ge, 2%As and (surprisingly!) 0.01%Cl are the most stable against nucleation.

3.2 The composition dependent extent of heterogeneity

Nucleation in glass is known to be usually *heterogeneous*, i.e., the nuclei tend to appear on the surface of a sample rather than distribute evenly in the volume. Note that only the case of homogeneous nucleation is considered in classical crystallization kinetics, a fact that creates additional problems when comparing theory with experiment for such non-classical objects like glass.

In order to evaluate heterogeneity in a numerical way, we have elaborated a simple method which includes the removal of the surface layer [61]. The main effect of the removal is the resection of the surface nuclei with the consequent rise of transparency. Next, the extent of heterogeneity *G* can be evaluated as:

$$G = (T_3 - T_2)/T_1 , \quad (2)$$

where T_1 is transparency (i.e., the optical transmission at 1000 cm^{-1}) for the as-prepared glass (of 15 mm thickness), T_2 is the transparency after ageing and T_3 is the transparency of the aged sample after the removal of the surface layer (0.5 mm from each side of the cylinder, a procedure that gives a sample of 14 mm thickness). The method is illustrated on the Se-Te series as an example in the left-top and left-bottom (Te) of Fig.8.

From Fig.8, it can be seen that the distribution of crystalline nuclei is most homogeneous in the Se-Ge system having G=0-0.2. The negative *G* for the 5%Ge sample may indicate the "inverse heterogeneity", a situation whereby nuclei prefer to burn within the volume rather than at the surface. The opposite deviation G>1, which is observed in the Se-Cl series for the 0.05%Cl sample when the volume becomes more transparent after ageing ($T_3 > T_1$), may be a result of the sample thinning. Another possibility, of *non-crystalline ordering* during ageing, seems to be more interesting. The reason for this ordering may be the development of the IReO regions in the glassy matrix (see the dotted line in Fig.2) without nucleation.

One can note a remarkable similarity in the *r(N)* graphs in Fig.5 for the as-prepared glasses and the *G(N)* graphs in Fig.8 for the aged glasses, and not only in the extrema location,

which coincides for every Se-X series, but also in the dependence shape which is qualitatively the same for the Se-Te, Se-As and Se-Cl series. For the Se-S and Se-Ge series, the shapes are somewhat different. One should note, however, that the Se-S glass is a special case because of the introduction of sulphur with T_g= -25°C, which would decrease the glass transition temperature in the series. Accordingly, Se-S glasses are especially inclined to crystallization when ageing at room temperature.

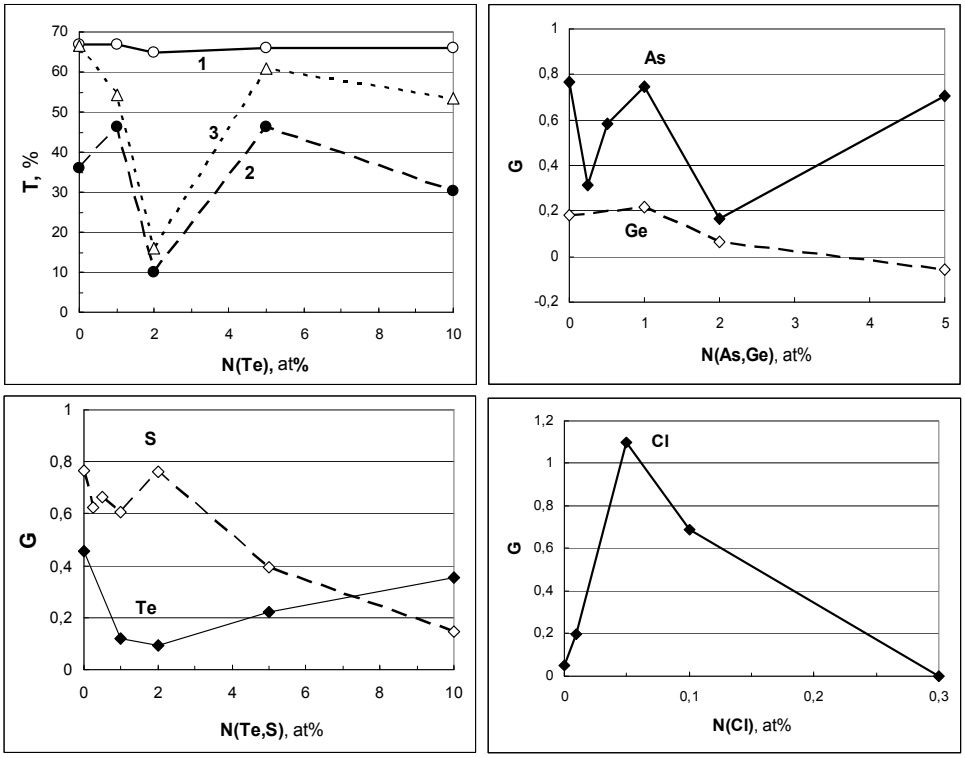

Fig. 8. The extent of heterogeneity, G by eq.(2), for spontaneous nucleation in Se-X glasses. T_i is the optical transmission at 1000 cm^{-1} for the as-prepared glass (1), the aged glass (2) and the aged glass without a surface layer (3).

In spite of these deviations, a non-trivial relation between the inclination to heterogeneous nucleation, *G(N)*, and a change in chemical bonding, reflecting by *r(N)*, is observed. Note that by means of the X-ray fluorescence method we probe only the *surface* layer of the sample; therefore, there exists a direct connection between *nucleation ability* and the *density of valence electrons*, with which the value of *r(N)* can be related. This is a direct route to hypervalent electron-rich bonds, which were discussed in section 2.3: the higher the electron density, the easier the formation of such HVBs representing active centres in covalent network, the centres which provide for processes including crystallization. The concentration of HVBs may be high owing to the decrease of energy when HVBs are associated (see Fig.4), probably in the form of bond waves. Thus, foreign atoms can interact strongly and non-linearly with the

bond waves which spread in non-crystalline network during the glass preparation (3D waves) and ageing (2D waves). What is a mechanism for such an interaction?

3.3 Non-linearity and self-organization in glass

From a phenomenological point of view, one can distinguish between "*impurity*" (non-linear) and "*component*" (smooth) concentration regions [54]. The boundary concentration, after which non-linearity begins to vanish, depends upon the system; it is about 2% for Se-S, Se-Te and Se-Ge glasses, about 1% for Se-As glasses, and about 0.05% for Se-Cl glasses (Figs.5-8). Let us discuss a possible nature of non-linearity in a low-concentration "impurity" region.

Starting from classical CRN [30], one cannot wait for any singularities except for those stipulated by a phase diagram, and it is generally accepted that foreign atoms enter into a CRN with "normal" valence (e.g., Te forms the **–**Se-Se-**Te**-Se-Se- chains), thus causing a proportional change in glass properties. The above-demonstrated non-linearity means that this is not the case and, hence, that the valence might be unusual. We have a model of *hypervalent bonds* - HVBs - after Dembovsky (section 2.3) for just this situation. It is clear, however, that the HVBs in a concentration of about 1% cannot explain the *macroscopic* effects observed. This is the *bond wave* model for the case of the collective interaction between "normal" bonds and HVBs. Next, the question about the nature of non-linearity should be reformulated: how do selenium bond waves interact with foreign atoms in a selenium network? Let us begin with the quantum-chemical modelling of the simplest case of Se-Te.

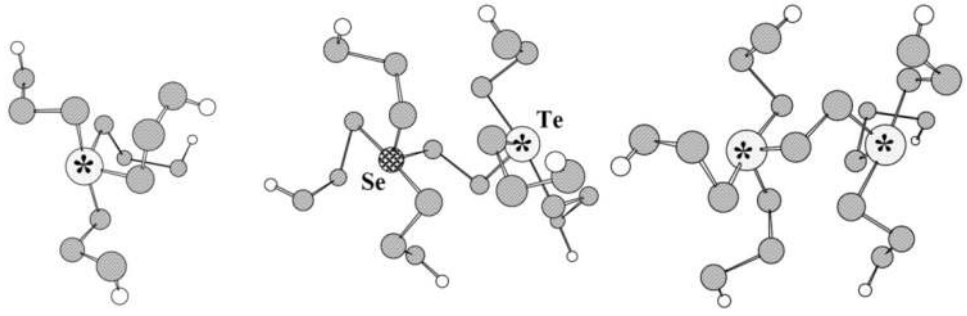

Fig. 9. A quantum-chemical modelling of HVBs in a selenium clusters containing Te atoms after [62]. The energies below are compared with the selenium CRN of the same size.

It can be seen in **Fig.9** that even a simple hypervalent Te_4^0 decreases the energy of the surrounding network (-0.23 eV). When the selenium wavefront (see d-layer in Fig.3, on the left) moves closer, a more stable $Se_4^0Te_4^0$ (-0.65 eV) is formed. Hence, a hypervalent Te atom represents an energetic trap for the selenium bond wave; however, this is so for only that local part of the wavefront, a part that interacts with the atom. When the Te concentration is high enough, the atoms can form hypervalent associates with the additional decrease in energy - see dimer 2(Te_4^0) in Fig.9.

The result of such an interaction is currently unclear. Given only the traps, foreign HVBs - such as Te_4^0 - should slow down or even destroy a bond wave, most probably to the extent that it is proportional to their concentration. However, we observe both maxima and minima in concentration dependencies in different Se-X series (Figs.5-8); hence, the interaction is not simple and depends on the concentration of foreign atoms. The reasons may be both in their bonding state and/or their arrangement – random or ordered. An ordered state can be realized by a directed diffusion of impurity under the action of any bond waves spreading through the melt, before the waves are frozen in solid glass.

The nature of the added atoms is also significant for their interaction with the bond wave. For example, a similar quantum chemical study for the Se-Cl system [63] leads to the same qualitative result as for with Se [52] and Se-Te [62], namely, the aggregation of HVBs with the participation of foreign atoms which leads to a lowering of energy – see **Fig.10** (chlorine atoms are chequered).

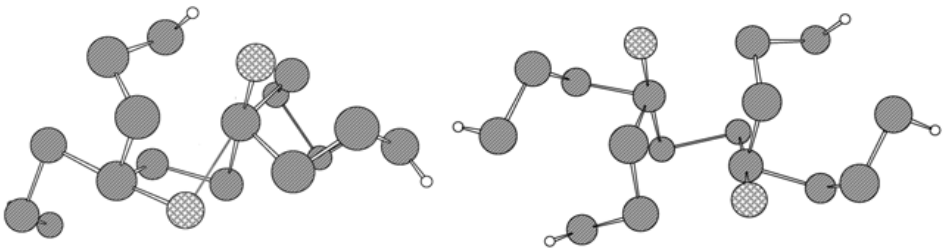

E= −0,57 eV **E= −0,37 eV**

Fig. 10. Two of the lowest energy complex HVBs in Se-Cl after [63].

The configurations and energies in the Se-Cl case differ from those of Se-Te (Fig.9); in this way, the specificity of foreign atoms is revealed. Note that in the left configuration of the lowest energy in **Fig.10**, the Cl_2Se_5 fragment has not only over-coordinated Cl (a two-coordinated instead of the usual one-coordinated state) but also five-coordinated Se, i.e. chlorine induces the most coordinated Se state obtained by us so far (see four-coordinated Se in Fig.4, Fig.9 and Fig.10, as well as the configurations with three-coordinated Se in other chalcogenide glasses [39]). One should note, however, that the relation between coordination and valence is not strictly determined, especially in the hypervalent case [64]. Indeed, by use of only the geometric arrangement, it is impossible to conclude does a chemical bonding exist between the atoms under consideration – this is the question to the quantum-chemistry study of a concrete configuration.

The method of adding foreign atoms in a simple non-crystalline matrix with the further comparison of experimental features with quantum-chemical models seems to be a fruitful way for understanding what is the nature of chemical bonding in glass formers and how one can creates various bonding states and/or structures. As to the structures, let us consider an additional feature that we found when investigating Se-X glasses by means of IR spectroscopy.

In **Fig.11** one can see a *narrow* absorption band at 792 cm^{-1} on the high-frequency side of the third overtone for the 245 cm^{-1} band of Se: the line half width is one-third of that for the overtone. Note that the 792 cm^{-1} band develops only for a definite concentration of chlorine,

existing in the sample 0.01%Cl, which is most persistent for nucleation (Fig.7), and in the sample 0.05%Cl, which has the greatest capacity for heterogeneous nucleation (Fig.8). Interestingly, the same 792 cm^{-1} band also observed in the Se-As series for the 0.25%As sample (compared with the minimal heterogeneity in Fig.8) and unexpectedly at 5%As [65] (one can also see the extrema at the same concentrations of 0.01-0.05%Cl and 0.025%As in other properties for fresh glasses in Fig.5). Hence, the *ordering* which reveals itself as the 792 cm^{-1} narrow band can be related to the selenium matrix, the structure of which is modulated by means of the impurity introduced into it. Interestingly, the ordering can manifest in properties in the opposite manner, depending upon the impurity, as it is seen in Fig.5 for the extrema at 0.01-0.05%Cl and 0.025%As .

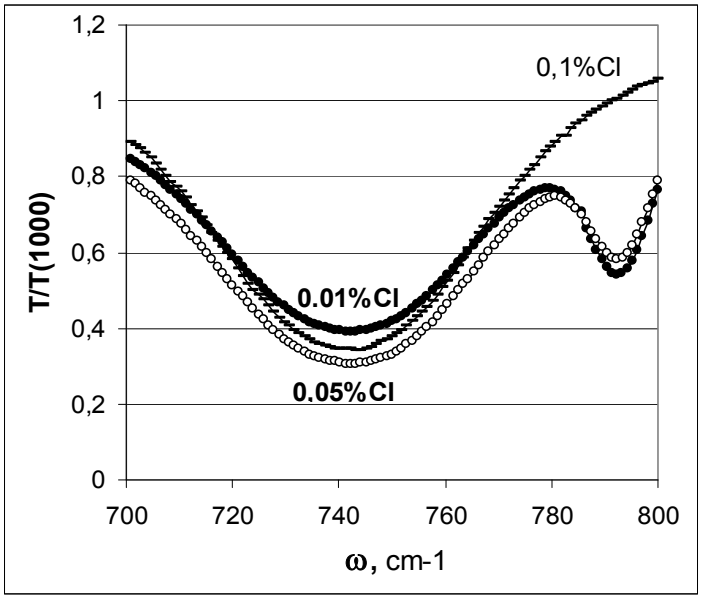

Fig. 11. IR spectra of Se-Cl glasses within the "phonon" range (400-1000 cm^{-1}) after [60]. *T* is the transmission at a given frequency, *T*(1000) is the transmission at 1000 cm^{-1}, i.e., the *transparency* (see Fig.7 and Fig.8).

When analysing the properties, a thoughtful reader can find out the disagreement in the *r*(0) values in Fig.5 and in the T_2/T_1 values in Fig.7 for pure selenium glass (X=0) in different Se-X systems, a fact that may devaluate the data itself. The explanation is rather simple: different series were formed in different regimes: the first regime was applied for Se-Te and Se-Ge, the second one for Se-As and Se-S, and the third one for Se-Cl. Indeed, Se glasses have similar properties in the series of the same preparation. This is the *memory effect*, which is well known for anyone who works with glasses.

The non-linearity, spontaneous ordering and the memory effect discussed above are signs of a *self-organizing* system, a system that possesses various scenarios for evolution, depending upon the system's nature and the information provided by external medium [66]. When glass is considered as a self-organizing system with bond waves as the basis for self-

organization, one acquires an appropriate tool not only for the explanation of the above-described phenomena but also for the planning of special experiments. In the following experiments, we use an external *information field* for governing the development of a glass structure by means of the directed spreading of bond waves in the region where they are most effective, i.e., at $T>T_g$ where 3D bond waves exist. Note that the above-described experiments concern nucleation in solid glass ($T>T_g$), a process that is provided by 2D bond waves spreading in the limits of frozen wavefronts. Thus, let us defreeze them.

4. The crystallization of softening glass in an ultrasonic field

4.1 Experimental conditions

The same Se-X series of glasses is used and optical transmission is also used as the general method for the observation of the crystallization process. The distinctions from the above experiments are as follows. First, the *temperature* range of the treatment 50-72°C is somewhat *above* the glass transition temperature T_g (which is about 35°C for Se), although the samples retain their form (in general). Second, the *time* of the treatment was 5-10 min instead of 5 years, as in the previous case. Third, the *ultrasonic field* is applied during treatment. Finally, the optical transmission was measured in *two directions* perpendicular to one another, before and after treatment.

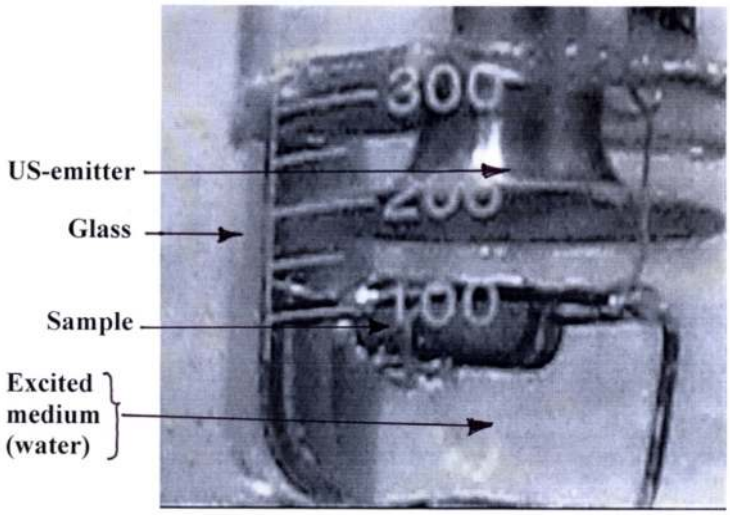

Fig. 12. The treatment of a Se-X sample in an ultrasonic field in a cavitation regime. Note the glass with water, the sample in the holder near the 100 ml mark and the end of a US-emitter at the 200 ml mark, as well as the large bubbles at the water's surface and near the sample.

In the framework of our understanding of glass as a self-organizing system, owing to the collective behaviour of hypervalent bonds in a covalent network, these conditions mean, first, the existence of 3D bond waves which activate *all of the volume* of a substance. Second, the crystallization process *accelerates* owing to not only the increase of the bond wave dimensionality but also of the bond wave velocity. Third, an ultrasonic field can play the

role of an *information field* that can orient bond waves. Finally, *anisotropy* can arise after the treatment.

The experimental equipment shown in **Fig.12** is rather simple: a glass with water (the excited medium for ultrasonic cavitation), in which the sample is placed in the holder. The sample has two pairs of perpendicular grains - A-A and B-B - the distance between like grains being equal: $d_{A\text{-}A}=d_{B\text{-}B}$. The US-emitter (its own frequency is 24 kHz and its vibration amplitude is 3 μ) is disposed at 10 mm above the upper grain A. The temperature varied from 50°C to 72°C and the time of treatment from 10 to 5 min. Note that the field is *weak*, having an intensity of about 0.2-0.3 W/cm^2 (the cavitation threshold is 0.1 W/cm^2). The vibration frequency in the excited medium is within the range of 1 kHz - 1 GHz, with a maximum at 5-10 MHz. At the end of treatment, the US-input is turned off, the emitter is lifted and the sample together with the holder is taken out of the glass with further cooling in the air down to room temperature. Then all the samples of a given Se-X series are subjected to optical investigation, which is performed at the same day.

The optical measurements were made in two directions: in the A-A direction along the axis of the US-emitter (i.e., through two "frontal" A grains, which are parallel to the emitter end in Fig.12) and in the B-B direction perpendicular to the emitter axis (one can see one of the lateral grains B facets in face in Fig.12). These directions are easily distinguished in the samples owing to the curve sides remaining after transformation of initial cylinders/tablets, which were used in the previous experiments at $T<T_g$, into the blocks using in the present experiments; the A-A grains correspond to the ends of the initial cylinders. The spectra were measured within the 400-5000 cm^{-1} range and the data up to 1000 cm^{-1} are discussed here. It may be desirable to catch the eye of future investigators to the 1000-5000 cm^{-1} interval: although we do not discuss the related data, it is a quite sensitive area for the observation of the crystallization process in the scale from 10μ to 2μ, respectively.

4.2 Basic experimental features

This study is currently in progress, although two articles describing experiments on the Se-As series [65] and Se-Te series [67] have just become available in English. Here, only basic experimental features are discussed; for additional information the reader is invited to look at the originals. Note that we use the optical transmission method for watching the crystallization process, which is again attributed primarily to the nucleation stage, a process that decreases transmission due to light scattering from a well-developed internal glass/crystal surface.

The first feature is a very fast darkening (for minutes) as compared with the previously considered darkening due to ageing (years). Thus, the first question is: what causes such rapid darkening? Temperature or cavitation?

It can be seen in **Fig.13** that even at 72°C - the highest temperature which was applied - the temperature itself has only a low effectiveness (compare the spectra 12 to 13) and only the US treatment strongly accelerates nucleation in softening glass (see spectrum 5 of a very low intensity).

The second feature is optical *anisotropy*, which is very weak in the initial glasses but can develop after US treatment. The anisotropy value in a given series depends on composition, as can be seen in **Fig.14** with Se-As as an example. Despite the series investigated, anisotropy always arises as a result of a strong darkening in the A-A direction together with a negligible change in transparency in the B-B direction. As to the anisotropy peak position,

a special concentration of 0.25%As in Fig.14 corresponds with the above-mentioned appearance of a narrow 792 cm^{-1} band - the same as that which is shown in Fig.11 for the Se-Cl series. This fact establishes a connection between the ability of pre-crystalline ordering in an as-prepared glass and the ability for the development of gigantic optical anisotropy in the glass after its further high-temperature treatment in an ultrasonic field.

In the framework of the bond wave model, anisotropy arises due to the definite location of an excitation source (see Fig.12): although one can suppose a nearly spherical distribution for the dissipation of the input energy in a cavitating medium, the input itself violates the symmetry. The excited medium, in addition, has a temperature above the glass transition temperature for the Se-X glasses investigated. Therefore, when an initially isotropic glass is placed into the cell (Fig.12), the bond waves - which were initially frozen in different directions, as in the case shown in the right-hand part of Fig.3 - begin to refreeze (2D→3D), and the refrozen bond wave will move in a definite direction, remaining this direction after glass cooling.

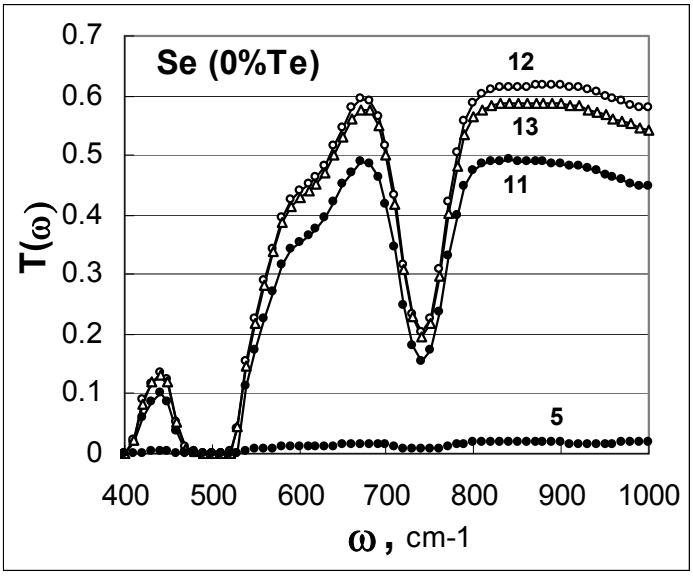

Fig. 13. Optical transmission spectra of the aged Se glass (11), the aged glass after polishing (12) and the polished glass after a 5 min treatment at 72°C (13). Curve 5 corresponds with the polished sample (an analogue of 12) after a 5 min treatment in a cavitation US field at the same temperature, 72°C. The measurements are made in the A-A direction.

The question is: in what direction will the refrozen bond waves move? It seems likely that the layers/wavefronts will be oriented in the A-A direction, parallel to the vibrating end of the US-emitter (see Fig.13). Insofar as crystallization begins within the layers containing active hypervalent bonds, then one obtains a system of partially-crystallized layers divided by periodic glass-like regions. This system is frozen in the sample after its removal from the cell with further quenching in the air. The sample reveals optical anisotropy (see line 5 in Fig.14) because in such a layered structure a measuring beam should scatter strongly when

it probes in the A-A direction (the beam falls onto the nucleated layers) and scatter much less in the B-B direction (the beam spreads within transparent glass-like regions between the layers, as like along the optical wire).

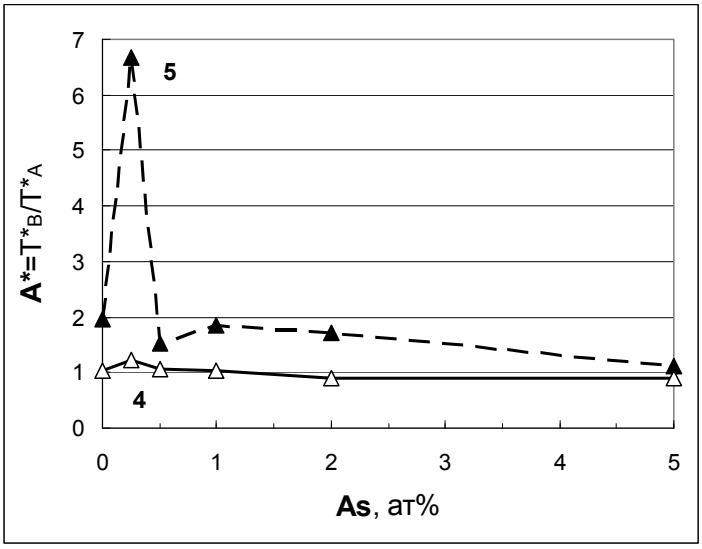

Fig. 14. The anisotropy in transparency (transmission at 1000 cm^{-1} measured in the A-A and B-B directions) for the Se-As series. The two lines correspond with the measurements before (4) and after (5) US treatment (72^0C, 5 min).

In an attempt to see the proposed internal structure, we used electron microscopy; the two images shown in **Fig.15** correspond to fresh fractures made in the two perpendicular directions.

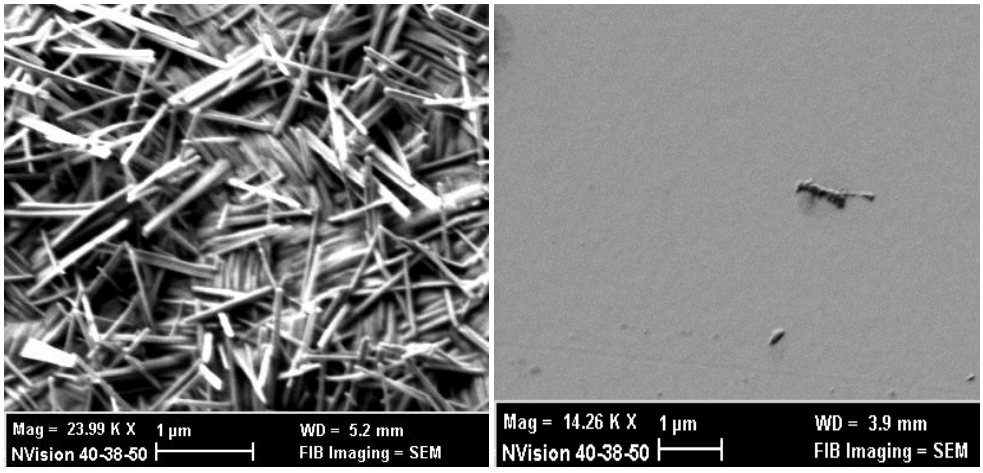

Fig. 15. A SEM image of the fracture made parallel to the A grain (on the left) and the B grain (on the right) for a selenium sample after US treatment at 72^oC.

In order to exclude the effects of many-component crystallization, we made the fractures using pure Se glass subjected to US treatment. This is that glass belonging to the Se-As series with the induced anisotropy of A*=2 (see 0% in Fig.14): after the US treatment, the transparency in the A-A direction was decreased doubly, while the transparency in the B-B direction was unchanged. In **Fig.15**, we present two images for the two fractures. The left image probably corresponds to the crystallized *d*-layer, along which a fracture developed. The right image looks like ordinary glass, probably corresponding to the glass-like region between the two adjacent *d*-layers.

For the crystallized layer (Fig.15, on the left) it is interesting to note the unusual *needle* form of nucleation in the selenium, which is known to be inclined to form the spheric-like crystallites. Of course, a much more intensive SEM investigation, as well as a wide set of other methods, is needed for a more adequate characterization of the materials obtained and, consequently, a deeper understanding of the processes involved in their formation. We hope that the described experiments of crystallization in glass under the action of impurities and/or ultrasonic field will help the coming investigators of glass and glass-ceramics in obtaining the new materials using non-traditional ways.

5. Conclusions

The structure of glass, considered from the chemical bond point of view using the bond wave model, acquires specific elements of order which develop during cooling (open system) owing to the alternation of chemical bonds (two-stable element) in the form of a bond wave (collective feedback between the elements). In the brackets, there are three general conditions for self-organization; they are naturally fulfilled in glass forming substances owing to their ability to form alternative hypervalent bonds. The processes in a self-organizing system proceed in a specific manner, and this is the reason why classic notions about crystallization works poorly in glass formers. On the other hand, self-organization opens new possibilities for both the understanding and management of related materials. One should note that although "self-organization in glass" becomes a hot topic (see [68] as an example), a real chemical bond is actually absent in the related works. We hope that our approach, connecting contemporary notions about chemical bonding - from the one side - and the self-organization theory (synergetics) - from the other side - will help to fill a significant gap in glass theory, including the understanding of the mechanism of glass-crystal transition and, in glass practice, the elaboration of new principles for the formation of glass-ceramic materials.

6. Acknowledgements

Dedicated to Prof. S. A. Dembovsky (1932-2010); his ideas and our long-term collaboration actually make him the co-author of this work.

This work was supported by the Russian Foundation of Basic Research (Grant No. 09-03-01158).

7. References

[1] J. Zarzycki. Glasses and the vitreous state. Cambridge University Press, Cambridge-New-York-Melbourne, 1991.

[2] P.T. Sarjeant, R. Roy. Mater. Res. Bull., 3, 265 (1968).
[3] D.R. Uhlmann. J. Non-Cryst. Solids, 7, 337 (1972).
[4] J.C.A. Vreeswijk, R.G. Gossink, J.M. Stevels. J. Non-Cryst. Solids, 16, 15 (1974).
[5] E. Ruckenstein, S.K. Ihm. J. Chem. Soc. Faraday Trans. I, 72, 764 (1976).
[6] G.F. Neilson, M.C. Weinberg. J. Non-Cryst. Solids, 34, 137 (1979).
[7] R.J.H. Gelsing, H.N. Stein, J.M. Stevels. Phys. Chem. Glasses, 7, 185 (1966).
[8] J.C.Th.G.M. Van der Wielen, H.N. Stein, J.M. Stevels. J. Non-Cryst. Solids, 1, 18 (1968).
[9] A.C.J. Havermans, H.N. Stein, J.M. Stevels. J. Non-Cryst. Solids, 5, 66 (1970).
[10] M.H.C. Baeten, H.N. Stein, J.M. Stevels. Silicates Industriels, 37, 33 (1972).
[11] G. Whichard, D.E. Day. J. Non-Cryst. Solids, 66, 477 (1984).
[12] W. Huang, C.S. Ray, D.E. Day. J. Non-Cryst. Solids, 86, 204 (1986).
[13] M.D. Mikhailov, A.C. Tver'janovich. Glass Phys. Chem., 6, No.5 (1980).
[14] M.D. Mikhailov, A.C. Tver'janovich. Glass Phys. Chem., 12, No.3 (1986).
[15] S.A. Dembovsky, L.M. Ilizarov, E.A. Chechetkina, A.Yu. Khar'kovsky. In: Proc. "Amorphous Semiconductors – 84". Gabrovo, Bulgaria, 1984. p.39.
[16] S.A. Dembovsky, L.M. Ilizarov, A.Yu. Khar'kovsky. Mater. Res. Bull. 21, 1277 (1986).
[17] S.A. Dembovsky, E.A. Chechetkina. Glass Formation (in Russ.). Nauka, Moscow, 1990.
[18] K.F. Kelton, A.L. Greer. J. Non-Cryst. Solids, 79, 295 (1986).
[19] S.A. Dembovsky. Zh. Neorg. Khim. (Russ. J. Inorg. Chem.), 22, 3187 (1977).
[20] S.A. Dembovsky. Proc. "Amorphous Semiconductors – 80". Kishinev, USSR, 1980. p.22.
[21] S.A. Dembovsky, E.A. Chechetkina. Mater. Res. Bull., 16, 606 (1981).
[22] S.A. Dembovsky, E.A. Chechetkina. Mater. Res. Bull., 16, 723 (1981).
[23] S.A. Dembovsky, E.A. Chechetkina. J. Non-Cryst. Solids 64, 95 (1984).
[24] V.M. Fokin, E.D. Zanotto, W.P. Schmelzer, O.V. Potapov. J. Non-Cryst. Solids, 351, 1491 (2005).
[25] J.L. Nowinski, M. Mroczkowska, J.E. Garbarczyk, M. Wasiucionek. Materials Science-Poland 24, 161 (2006).
[26] A.H. Moharram, A.A. Abu-sehly et al. Physica B, 324, 344 (2002).
[27] L. Berthier. Physics 4, 42 (2011).
[28] P.N. Pusley, E. Zaccarelli et al. Phil. Trans. R. Soc. A, 367, 4993 (2009).
[29] H. Tanaka. J. Phys.: Condens. Matter, 23, 284115 (2011).
[30] W.H. Zachariasen. J. Amer. Ceram. Soc., 54, 3841(1932).
[31] G. Biroli. Sèminaire Poincarè XII, 37 (2009).
[32] S.A. Dembovsky. Mater. Res. Bull., 16, 1331 (1981).
[33] N.A. Popov. JETP Lett., 31, 409 (1980).
[34] S.A. Dembovsky, E.A. Chechetkina. J. Non-Cryst. Solids, 85, 346 (1986).
[35] S.A. Dembovsky, E.A. Chechetkina. Philos. Mag., B53, 367 (1986).
[36] S.A. Dembovsky, E.A. Chechetkina. J. Optoel. Adv. Mater., 3, 3 (2001).
[37] S.A. Dembovsky. J. Non-Cryst. Solids, 353, 2944 (2007).
[38] E.A. Chechetkina. J. Optoel. Adv. Mater., 13, 1385 (2011).
[39] S.A. Dembovsky, A.S. Zyubin. Russ. J. Inorg. Chem., 46, 121 (2001).
[40] S.A. Dembovsky, A.S. Zyubin, O.A. Kondakova. Mendeleev Chemistry Journal (Zhurnal Ross. Khim. Ob-va im.D.I.Mendeleeva), 45, 92 (2001).
[41] S. Zyubin, F.V. Grigoriev, S.A. Dembovsky. Russ. J. Inorg. Chem., 46, 1350 (2001).
[42] J.L. Muscher. Angew. Chem. Int. Ed., 8, 54 (1969).
[43] W.B. Jensen. J. Chem. Educ., 83, 1751 (2006).

[44] G. Pimentel. J. Chem. Phys., 19, 446 (1981).
[45] S.C. Moss, D.L. Price. In: Physics of Disordered Materials (Eds. D. Adler, H. Fritzsche, S.R. Ovshinsky), Plenum, New York, 1985. p.77.
[46] E.A. Chechetkina. J. Phys.: Condes. Matter, 7, 3099 (1995).
[47] E.A. Chechetkina. Solid State Commun., 87, 171 (1993).
[48] E.A. Chechetkina. In: Proc XVII Inter. Congr. Glass, Beijing, 1995. vol.2, p.285.
[49] E.A. Chechetkina. J. Non-Cryst. Solids, 128, 30 (1991).
[50] E.A. Chechetkina. In: Fractal Concepts in Materials Science. MRS Proc., vol.367 (1995).
[51] E.A. Chechetkina. J. Non-Cryst. Solids, 201, 146 (1996).
[52] S.A. Dembovsky, A.S. Zyubin. Russ. J. Inorg. Chem. 54, 455 (2009).
[53] M. Kastner, D. Adler, H. Fritzsche. Phys. Rev. Lett. 37, 1504 (1976).
[54] S.A. Dembovsky, E.A. Chechetkina, T.A. Kupriyanova. Materialovedenie (Mater. Sci. Trans.), No.4, 37 (2004).
[55] M.F. Kotkata, E.A. Mahmoud, M.K. El-Mously. Acta Phys. Acad. Sci. Hung., 50, 61 (1981).
[56] M.F. Kotkata, M.K. El-Mously. Acta Phys. Hung., 54, 303 (1983).
[57] G. Parthasarathy, K.J. Rao, E.S.R. Gopal. Philos. Mag., B50, 335 (1984).
[58] S.A. Dembovsky, L.M. Ilizarov, A.Yu. Khar'kovsky. Mater. Res. Bull., 21, 1277 (1986).
[59] M. Hansen, K. Anderko. Constitution of Binary Alloys. McGraw-Hill, 1958.
[60] E.A. Chechetkina, A.B. Vargunin, V.A. Kuznetzov, S.A. Dembovsky. Materialovedenie (Mater. Sci. Trans.), No.7, 28 (2006).
[61] E.A. Chechetkina, E.B. Kryukova, A.B. Vargunin. Materialovedenie (Mater. Sci. Trans.), No.6, 29 (2007).
[62] A.S. Zyubin, E.A. Chechetkina, S.A. Dembovsky. Russ. J. Inorg. Chem., 57, 913 (2012).
[63] S. Zyubin, S.A. Dembovsky. Russ. J. Inorg. Chem., 56, 329 (2011).
[64] D.W. Smith. J. Chem. Educ., 82, 1202 (2005).
[65] E.A. Chechetkina, E.V. Kisterev, E.B. Kryukova, A.I. Vargunin. Inorg. Mater.: Appl. Res., 2, 360 (2011).
[66] H. Haken. Information and Self-Organization. A macroscopic Approach to Complex Systems. Springer, 1988, 2000, 2006.
[67] E.A. Chechetkina, E.V. Kisterev, E.B. Kryukova, A.I. Vargunin. J. Optoel. Adv. Mater., 11, 2034 (2009).
[68] P. Boolchand, G. Lucovsky, J.C. Phillips, M.F. Thorpe. Philos. Mag., 85, 3823 (2005).